Dispersion Analysis within a Measured 1,4 km MIMO Multimode Channel

Andreas Ahrens, Steffen Schröder and Steffen Lochmann
Hochschule Wismar, University of Technology, Business and Design, Philipp-Müller-Straße 14, 23966 Wismar, Germany

Keywords: Multiple-Input Multiple-Output System, Optical Fibre Transmission, Multimode Fiber (MMF), Modal Dispersion, Chromatic Dispersion.

Abstract: In this contribution a signal theoretic Multiple Input Multiple Output (MIMO) system model for estimating modal and chromatic dispersion is developed. Based on channel measurements within a 1,4 km MIMO multimode channel parameters for modal and chromatic dispersion are estimated. Furthermore, taking given parameters of the dispersion into account, the introduced signal theoretic MIMO system model enables a reconstruction of the MIMO specific impulse responses.

1 INTRODUCTION

The increasing desire for communication and information interchange has attracted a lot of research since Shannon's pioneering work in 1948.

A possible solution was presented by Teletar and Foschini in the mid 90's, which revived the MIMO (multiple-input multiple-output) transmission philosophy introduced by van Etten in the mid 70's (Telatar, 1999; Foschini, 1996; van Etten, 1975; van Etten, 1976).

Since the capacity of wireless multiple-input multiple-output (MIMO) systems increases linearly with the minimum number of antennas at both, the transmitter as well as the receiver side, MIMO schemes have attracted substantial attention (Zhou et al., 2005; Mueller-Weinfurtner, 2002) and can be considered as an essential part of increasing both the achievable capacity and integrity of future generations of wireless systems (Kühn, 2006; Zheng and Tse, 2003). MIMO transmission has influenced nearly any standard of wireless communication.

However, the MIMO principle is not limited to wireless communication channel and a lot of scenarios can be described by the MIMO technology (Kühn, 2006; Bülow et al., 2011; Singer et al., 2008).

Within the last years, the concept of MIMO (multiple input multiple output) transmission over multimode and multicore fibers has attracted increasing interest in the optical fiber transmission community, e. g. (Bülow et al., 2010; Bülow et al., 2011; Singer et al., 2008), targeting at increased fiber capacity.

Usually, the fibre capacity is limited by the dispersion. In multimode fibres the modal dispersion dominates the chromatic dispersion by orders. Only systems with Restricted Mode Launching (RML), e. g. the 10 Gbit Ethernet system standard 10GBASE-SR, focus on the description of both dispersion effects(Pimpinella et al., 2011; Castro et al., 2012).

Since the modal and the chromatic dispersion are considered to be independent, the system impulse response is given by the convolution of these individual impulse responses.

Against this background, the novel contribution of this paper is that based on channel measurement with a 1,4 km multimode fibre, a signal theoretic MIMO system model for estimating modal and chromatic dispersion is developed.

By taking given parameters of the dispersion into account, the introduced system model enables a reconstruction of the MIMO specific impulse responses. Thus, a fundamental algorithm for further studies on the impact of dispersion and for a comparison of different MIMO systems utilizing different wavelengths is presented.

The remaining part of this contribution is organized as follows: Section 2 introduces our system model. The measurement setup for estimating the channel impulse responses is presented in section 3. In section 4 our signal theoretic system model is introduced and discussed. The associated performance results are presented and interpreted in section 5. Finally, section 6 provides our concluding remarks.

Ahrens A., Schröder S. and Lochmann S..
Dispersion Analysis within a Measured 1,4 km MIMO Multimode Channel.
DOI: 10.5220/0004495203910397
In *Proceedings of the 4th International Conference on Data Communication Networking, 10th International Conference on e-Business and 4th International Conference on Optical Communication Systems* (OPTICS-2013), pages 391-397
ISBN: 978-989-8565-72-3

2 MULTIMODE MIMO CHANNEL

In order to form the optical MIMO channel, different sources of light have to be launched into the multimode fibre. In this work a (2×2) optical multimode MIMO channel is studied. The corresponding electrical MIMO system model is highlighted in Fig. 1.

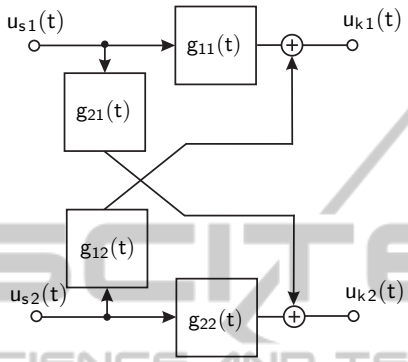

Figure 1: Electrical MIMO system model (example: $n = 2$).

In Fig. 2 the optical MIMO setup is shown schematically. On the left side the transmitter side is represented for launching different sources of light into the fibre. By coupling light in the center of the multimode core, described by TX_1, low-order mode groups are activated (e. g. fundamental mode). For activating high order mode groups, described by TX_2, light has to be launched into the fibre with an given eccentricity.

At the receiver side, different spatial filters are used to separate the different mode groups. For low-order mode groups the spot filter (described by RX_1) and for higher order mode groups the ring filter is used (described by RX_2). Together with the mode group coupling along the 1,4 km long fibre, the MIMO system model according to Fig. 1 can be formed (Pankow et al., 2011).

3 MEASUREMENT SETUP

In order to evaluate the potential of MIMO in the field of optical multimode communication channels, a good knowledge of the MIMO specific impulse responses and their corresponding dispersion parameter is needed. For analyzing the MIMO specific impulse responses, the measurement setup depicted in Fig. 3 is used. For measuring the impulse responses, the input impulse was generated by using the Picosecond Diode Laser System (PiLas). For the measurement

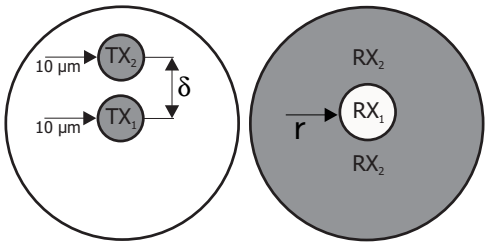

Figure 2: Forming the optical MIMO channel (left: light launch positions at the transmitter side with a given eccentricity δ, right: spatial configuration at the receiver side as a function of the mask diameter r).

campaign two different laser diodes are used: The spectral properties of each laser diode are determined by measurement. The first laser diode has a center wave length (CWL) of 1326 nm and a spectral half width of approximately 8 nm. The second laser diode has a CWL of 1576 nm and a spectral half width of approximately 10 nm. Fig. 4 shows exemplarily the

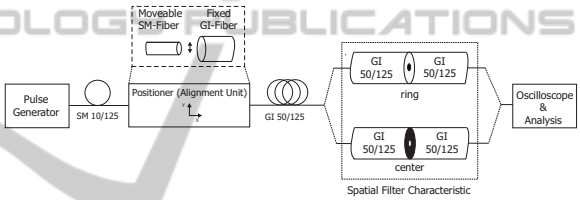

Figure 3: Measurement setup for measuring the MIMO specific impulse responses.

measured spectrum of the 1576 nm Fabry-Perot laser with the typical modal structure.

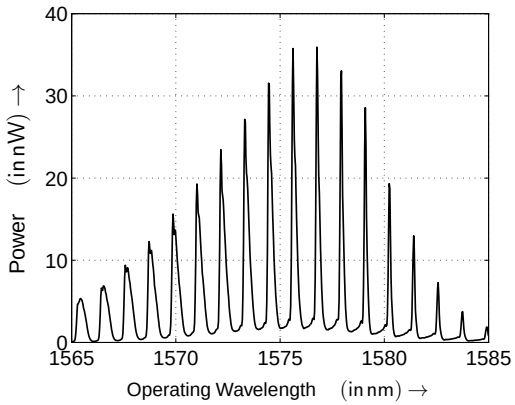

Figure 4: Spectrum of used Fabry-Perot Laser (resolution bandwidth (RBW) of optical spectrum analyzer 0,07 nm).

For generating a MIMO system, different sources of light have to be launched into the multimode fibre. For the measurement campaign the laser light will be launched through a single mode waveguide

into the core of a multimode waveguide. For the (2×2) MIMO System two different sources of light are needed. This part is realized by the first coupler component using a splicer. In a splicer the end of the transmitter waveguide and the beginning of the transmission path are clamped together where they are aligned exactly to each other (Fig. 5). By using the center launch condition only the fundamental mode is stimulated, represented by the signal $u_{s1}(t)$ in Fig. 1. The signal $u_{s2}(t)$ in Fig. 1 represents the offset launch condition for activating higher order mode groups. For the measurements an eccentricity of $10\,\mu$ m was chosen. As a transmission channel a graded-index fibre of 1,4 km length was chosen. At the receiver side,

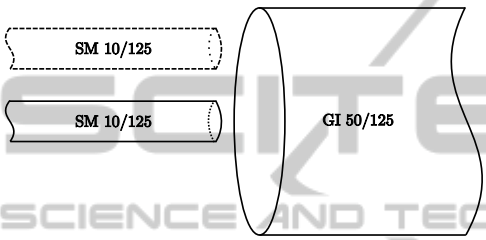

Figure 5: Transmitter side configuration with center and offset light launch condition.

for separating the different optical channels, different spatial filters (i. e, the spot filter with a diameter of $r = 15\,\mu$m for low order mode groups and the corresponding ring filter for higher order mode groups) are used (Fig. 6). These spatial filters have been produced by depositing a metal layer at fibre end-faces and subsequent ion milling (Pankow et al., 2011; Aust et al., 2012). To determine the appropriate impulse response for the respective channel, the particular transmitter/receiver combination has to be chosen.

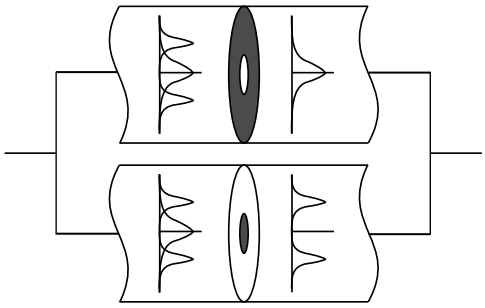

Figure 6: Receiver side filter configuration for separating the different channels.

Fig. 7 highlights the electrical impulse for measuring the MIMO-specific impulse responses. The pulses are chosen in a way that the same optical power is coupled into the multimode fibre core. Theoretically, an impulse like a dirac delta pulse has to be chosen in order to measure the channel impulse response unaffectedly from the input impulse. However, in this case the optical power is no longer sufficient to make the modal structure measurable. Thus, the input impulses shown in Fig. 7 are a good compromise to an impulse like a dirac delta impulse at a reasonable amount of coupled transmit power. The MIMO-specific impulse responses are obtained after deconvolution with the measured impulse responses.

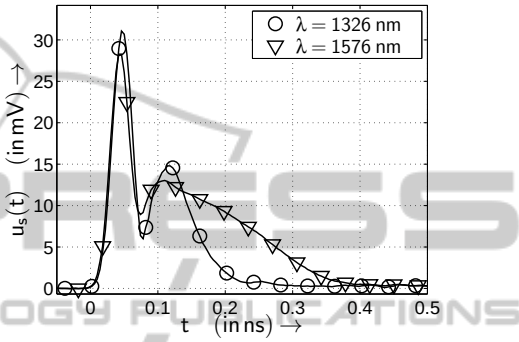

Figure 7: Input impulse for calculating the MIMO-specific impulse responses at different operating wavelength.

4 SIGNAL THEORETIC SYSTEM MODEL

The limiting factor in transmitting high speed data over single input single output (SISO) multimode fibers is modal and chromatic dispersion. In order to be able to study the effect of modal and chromatic dispersion especially in MIMO communication, a simplified SISO system model is developed, which takes the modal as well as the chromatic dispersion of a multimode fibre into account. Thereby the individual mode groups, which propagate along the fibre with different speed, are modeled as a Gaussian impulse sequence as highlighted in Fig. 8. This sequence is described mathematically as

$$g(t) = \sum_{\ell=0}^{q-1} a_\ell \, \delta(t - \tau_\ell) \qquad (1)$$

by taking q dominant mode groups into account which propagate along the fibre. The delay time of each mode group is described τ_ℓ and the mode group dependent weighting factor by a_ℓ.

Since the modal as well as the chromatic dispersion are independent from each other, the gaussian impulse sequence can be decomposed into two parts: a weighted dirac delta impulse response $g_m(t)$ for the

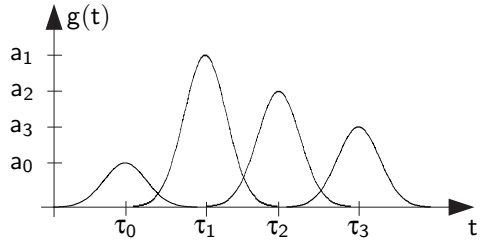

Figure 8: Approximated impulse responses.

description of the modal dispersion (Fig. 9) and a common gaussian part $g_c(t)$ for the description of the chromatic dispersion (Fig. 10). The resulting SISO specific impulse response can be obtained by convolution of $g_m(t)$ and $g_c(t)$ and results in:

$$g(t) = g_m(t) * g_c(t) \quad . \tag{2}$$

Fig. 8 shows an exemplarily impulse response de-

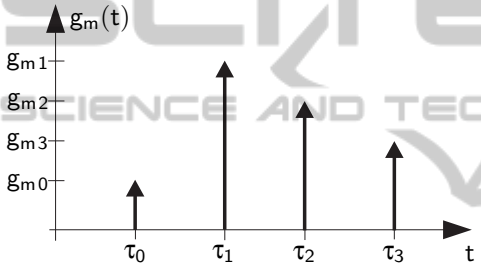

Figure 9: Weighted Dirac delta impulse pulse response for the description of the SISO specific mode dispersion.

composed into individual gaussian impulses. In this work it is assumed that all mode groups are described by Gaussian impulses with individual delay and spread parameters. This sequence of weighted Gaussian pulses can now be decomposed into a sequence weighted dirac impulses (Fig. 9), for the description of the modal dispersion, and into a Gaussian pulse (Fig. 10), for the description of the chromatic dispersion.

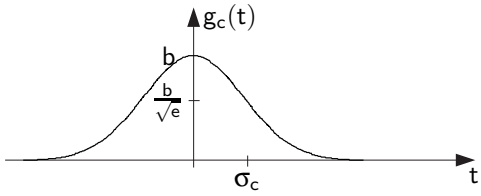

Figure 10: Gaussian pulse to describe chromatic dispersion.

Fig. 9 and 10 also highlights the parameters of the presented SISO system model. The parameter τ_ℓ describes the average delay time for the mode group ℓ, $g_{m\ell}$ is the amplitude of ℓth mode group and σ_c describes the spread of each mode group, which is assumed to be the same for all mode groups.

4.1 Modal Dispersion

When launching light into the fibre, different mode groups will be activated which propagate along the fibre with different speed and different attenuation. This effect can be described by a sum of weighted dirac delta impulses as shown in Fig. 9. Taking the q dominant mode groups into account, the mode dispersion is described by the following impulse response

$$g_m(t) = \sum_{\ell=0}^{q-1} g_{m\ell}\,\delta(t-\tau_\ell) \tag{3}$$

with the parameter τ_ℓ as the delay time and the parameter $g_{m\ell}$ as the weighting coefficient of the ℓ-th mode group.

The amount of modal dispersion included in the measured impulse response can now be described according to wireless transmission channels by a delay spread parameter σ_m (Pätzold, 2002). The parameter σ_m describes the spread of the whole impulse response and can be used as a reference value for the modal dispersion. The delay spread is given by:

$$\sigma_m = \sqrt{\frac{1}{A}\sum_{\ell=0}^{q-1}(\tau_\ell g_{m\ell})^2 - (\bar{t}_m)^2} \quad . \tag{4}$$

Therein, the average delay of all modal groups (i. e.$\bar{t}_m$) results in

$$\bar{t}_m = \frac{1}{A}\sum_{\ell=0}^{q-1}\tau_\ell\,(g_{m\ell})^2 \tag{5}$$

with normalization parameter $A = \sum_{\ell=0}^{q-1}(g_{m\ell})^2$. With this normalization parameter, the mode-group dependent weighting coefficients fulfil the boundary condition

$$\frac{1}{A}\sum_{\ell=0}^{q-1}(g_{m\ell})^2 = 1 \quad . \tag{6}$$

4.2 Chromatic Dispersion

Theoretically, in the absent of chromatic dispersion, each mode group can be described by a single dirac delta impulse with a mode dependent delay and weighting factor. However, as the operating wavelength increased, the modes within a mode group travel with different speed and therefore the delay time between the different modes within a mode group become visible. This results in a broadening of the beforehand analyzed individual mode group dirac delta impulses. The parameter for this widening is the spread parameter σ_c. However, through the widening of the mode group dependent dirac delta impulses, the amplitude of impulse response is also weighted, i.e.,

the amplitude of impulse response a_ℓ and the modal dependent weighting factors $g_{\mathrm{m}\ell}$ depend on the parameter σ_c.

The chromatic dispersion of each mode group is described by a normalized Gaussian impulse (Fig. 10) and is given as

$$g_\mathrm{c}(t) = \frac{1}{\sigma_\mathrm{c}\sqrt{2\pi}}\,\mathrm{e}^{-\frac{t^2}{2\sigma_\mathrm{c}^2}} \tag{7}$$

The parameter b in Fig. 10 represents the normalization factor of the Gaussian impulse and results in

$$b = \frac{1}{\sigma_\mathrm{c}\sqrt{2\pi}} \ . \tag{8}$$

4.3 Spread Parameters

For the SISO system model, modal and chromatic dispersion are described by their corresponding spread parameters. Assuming that the individual mode groups are described as Gaussian pulses

$$g(t) = \sum_{\ell=0}^{q-1} a_\ell\,\delta(t-\tau_\ell) \ , \tag{9}$$

the parameter a_ℓ is obtained by combining (3) and (7) and results in

$$a_\ell = g_{\mathrm{m}\ell}\,\frac{1}{\sigma_\mathrm{c}\sqrt{2\pi}} \ . \tag{10}$$

Taking this equation into account, the mode group dependent weighting factor $g_{\mathrm{m}\ell}$ can be obtained as

$$g_{\mathrm{m}\ell} = a_\ell\,\sigma_\mathrm{c}\,\sqrt{2\pi} \tag{11}$$

by taking into account that the measured amplitude a_ℓ contains the information about the width of the gaussian pulse (i. e. chromatic dispersion) as well as the mode-dependent weighting factor. Therefore, the weighting factor $g_{\mathrm{m}\ell}$ can be determined with the predetermined spread parameter σ_c and the measured amplitude a_ℓ, i. e.

$$g_{\mathrm{m}\ell} = a_\ell\,\sigma_\mathrm{c}\,\sqrt{2\pi} \ . \tag{12}$$

Since the weighting of each mode group is described by the modal dispersion completely, the chromatic dispersion corresponding spread parameter σ_c can be calculated by taking the measured amplitudes a_ℓ into account.

4.4 MIMO System Model

In this work a $(2\times 2$ MIMO system model is investigated and the beforehand introduced signal theoretic SISO system model has now to be extended to the MIMO system model. The corresponding electrical MIMO system model is highlighted in Fig- 1 with the four existing transmission paths $g_{\nu\mu}(t)$ (with $\nu = 1,2,\ldots,n_\mathrm{R}$ and $\mu = 1,2,\ldots,n_\mathrm{T}$), which will be measured and analyzed separately. The number of transmitters is given by the n_T and the number of receivers by n_R, respectively. Therefore, the impulse response is given by

$$g_{\nu\mu}(t) = g_\mathrm{m}^{(\nu\mu)}(t) * g_\mathrm{c}^{(\nu\mu)}(t) \ . \tag{13}$$

According to equation (14) the modal dispersion can be described by

$$g_\mathrm{m}^{(\nu\mu)}(t) = \sum_{\ell=0}^{q-1} g_{\mathrm{m}\ell}^{(\nu\mu)}\,\delta(t-\tau_\ell^{(\nu\mu)}) \tag{14}$$

with the delay of ℓth mode group $\tau_\ell^{(\nu\mu)}$ and the corresponding weighting factors $g_{\mathrm{m}\ell}^{(\nu\mu)}$. The average delay of the mode groups can be calculated by

$$\bar{t}_\mathrm{m}^{(\nu\mu)} = \frac{1}{A^{(\nu\mu)}}\sum_{\ell=0}^{q-1}\tau_\ell^{(\nu\mu)}\left(g_{\mathrm{m}\ell}^{(\nu\mu)}\right)^2 \tag{15}$$

with the normalization factor $A = \sum_{\ell=0}^{q-1}\left(g_{\mathrm{m}\ell}^{(\nu\mu)}\right)^2$ (Pätzold, 2002). Finally, the modal dispersion results in:

$$\sigma_\mathrm{m}^{(\nu\mu)} = \sqrt{\frac{1}{A^{(\nu\mu)}}\sum_{\ell=0}^{q-1}\left(\tau_\ell^{(\nu\mu)}\cdot g_{\mathrm{m}\ell}^{(\nu\mu)}\right)^2 - \left(\bar{t}_\mathrm{m}^{(\nu\mu)}\right)^2} \ . \tag{16}$$

Assuming that the same laser is used for measuring all four impulse responses, the chromatic dispersion can be considered to be same within all four transmission path. Taking (7) into account, the following equation holds

$$g_\mathrm{c}^{(\nu\mu)}(t) = g_\mathrm{c}(t) \ . \tag{17}$$

5 RESULTS

Within this paper, channel measurements within a $1,4$ km (2×2) MIMO system are carried out. For the investigated optical MIMO channel an eccentricity δ of $10\,\mu$m and a mask diameter r of $15\,\mu$m were chosen (Fig. 2). Fig. 11 shows the four impulse responses for an operating wavelength of 1326 nm according to Fig. 1. Compared to 1576 nm depicted in Fig. 12 the influence of the chromatic dispersion is highly visible.

The impulse responses are obtained after deconvolution with the input impulse depicted in Fig. 7. Furthermore it is assumed that each optical input within

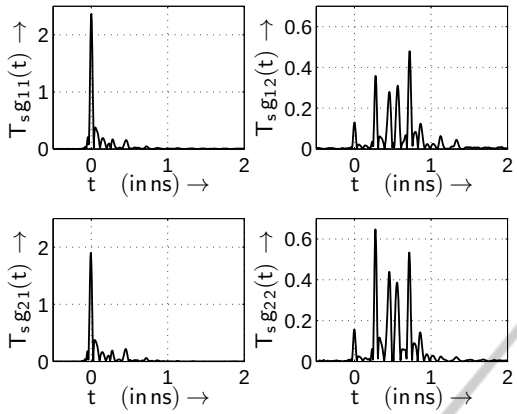

Figure 11: Measured electrical MIMO impulse responses with respect to the pulse frequency $f_T = 1/T_s = 5{,}00$ GHz at 1326 nm operating wavelength.

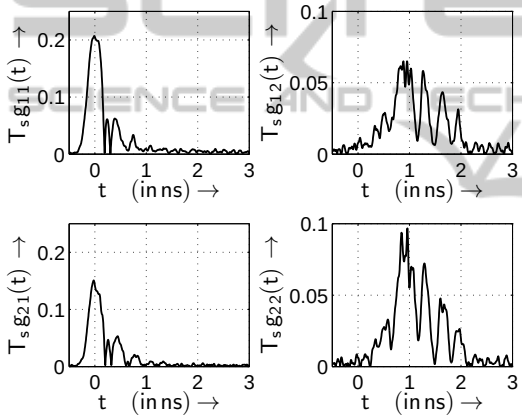

Figure 12: Measured electrical MIMO impulse responses with respect to the pulse frequency $f_T = 1/T_s = 5{,}00$ GHz at 1576 nm operating wavelength.

the multimode fiber will be fed by a system with identical mean properties with respect to transmit filtering and pulse frequency $f_T = 1/T_s$. For numerical assessment within this paper, the pulse frequency is chosen to be $f_T = 5{,}00$ GHz Taking the measured impulse

Table 1: Parameters of the calculated chromatic dispersion.

λ (in nm)	σ_c in (ps)
1326	15
1576	129

responses, depicted in Fig. 11 and 12, into account, the obtained parameters for the chromatic dispersion are presented in Tab. 1. For the same operating wavelength, the chromatic dispersion is assumed to be the same for all propagation paths and all individual mode groups. For comparison reason, the chromatic dispersion can be approximated by the following equation

$$\tau_c = D_c \, \delta_\lambda \, \ell \ . \tag{18}$$

The impulse spread τ_c can be described as the width of each impulse or mode group, measured at a 50% decay of the maximum amplitude and to be assumed to be approximately twice as large as the calculated spread parameter σ_c. The dispersion parameter D_c at the operating wavelength of 1576 nm can be assumed to be 20 ps/(nm km) (Senior, 2008). Together with the length of the measured multimode fibre of $\ell = 1{,}4$ km and the spectral width δ_λ (FWHW, Full Width Half Maximum) of the laser diode of 10 nm, an impulse spread τ_c of approximately 280 ps is obtained. With $\tau_c \approx 2\sigma_c$ the measured values of σ_c can be justified. At a operating wavelength of 1326 nm the chromatic dispersion tends to be zero. At this particular operating wavelength no chromatic dispersion appears. Therefore, at the operating wavelength of 1326 nm, the chromatic dispersion is not exactly zero, but much lower compared with an operating wavelength of 1576 nm.

The estimated parameters of the modal dispersion are highlighted in Tab. 2.

Table 2: Parameters of the calculated modal dispersion.

λ (in nm)	σ_c (in ps)			
-	$g_{11}(t)$	$g_{12}(t)$	$g_{21}(t)$	$g_{22}(t)$
1326	38	215	62	199
1576	159	424	185	353

Next to analyzed parameters of modal and chromatic dispersion, the introduced system model enables a reconstruction of the MIMO specific impulses responses by taking the estimated dispersion parameters into account. In Fig. 13 and 14 the approximated impulse response $g_{22}(t)$ is shown exemplarily at different operating wavelength by using the beforehand introduced system model and the estimated parameters of modal and chromatic dispersion. As shown by Fig. 13 and 14 the approximated impulse responses show a good correlation with the measured impulse responses.

6 CONCLUSIONS

Based on channel measurements, in this work a signal theoretic MIMO system model for estimating modal and chromatic dispersion is introduced and parameters for modal and chromatic dispersion for an 1,4 km multimode MIMO channel are estimated.

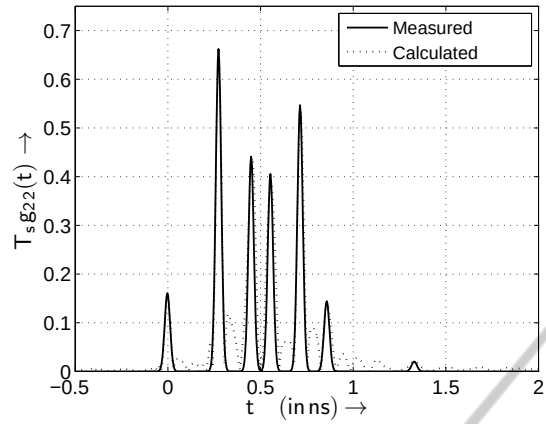

Figure 13: Calculated and measured impulse response $g_{22}(t)$ at 1326 nm operating wavelength.

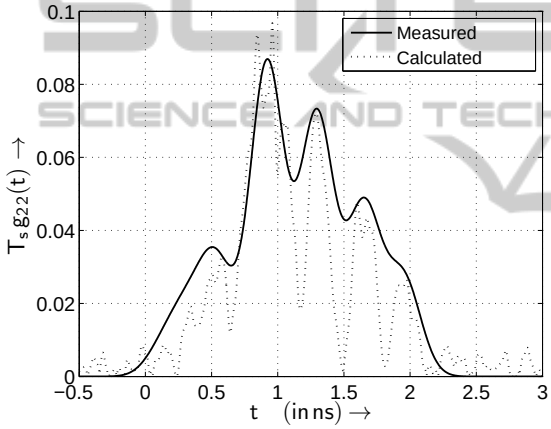

Figure 14: Calculated and measured impulse response $g_{22}(t)$ at 1326 nm operating wavelength.

ACKNOWLEDGEMENTS

The authors wish to thank their co-worker, Mr. Ralph Bornitz, for supporting the measurement campaign.

REFERENCES

Aust, S., Ahrens, A., and Lochmann, S. (2012). Channel-Encoded and SVD-assisted MIMO Multimode Transmission Schemes with Iterative Detection. In *International Conference on Optical Communication Systems (OPTICS)*, pages 353–360, Rom (Italy).

Bülow, H., Al-Hashimi, H., and Schmauss, B. (2010). Stable Coherent MIMO Transport over Few Mode Fiber Enabled by an Adiabatic Mode Splitter. In *European Conference and Exhibition on Optical Communication (ECOC)*, page P4.04, Torino, Italy.

Bülow, H., Al-Hashimi, H., and Schmauss, B. (2011). Coherent Multimode-Fiber MIMO Transmission with Spatial Constellation Modulation. In *European Conference and Exhibition on Optical Communication (ECOC)*, Geneva, Switzerland.

Castro, J., Pimpinella, R., Kose, B., and Lane, B. (2012). The Interaction of Modal and Chromatic Dispersion in VCSEL based Multimode Fiber Channel Links and its Effect on Mode Partition Noise. In *61th International Wire & Cable Symposium (IWCS)*, pages 724–730, Providence, Rhode Island, USA.

Foschini, G. J. (1996). Layered Space-Time Architecture for Wireless Communication in a Fading Environment when using Multiple Antennas. *Bell Labs Technical Journal*, 1(2):41–59.

Kühn, V. (2006). *Wireless Communications over MIMO Channels – Applications to CDMA and Multiple Antenna Systems.* Wiley, Chichester.

Mueller-Weinfurtner, S. H. (2002). Coding Approaches for Multiple Antenna Transmission in Fast Fading and OFDM. *IEEE Transactions on Signal Processing*, 50(10):2442–2450.

Pankow, J., Aust, S., Lochmann, S., and Ahrens, A. (2011). Modulation-Mode Assignment in SVD-assisted Optical MIMO Multimode Fiber Links. In *15th International Conference on Optical Network Design and Modeling (ONDM)*, Bologna (Italy).

Pätzold, M. (2002). *Mobile Fading Channels.* Wiley, Chichester.

Pimpinella, R., Castro, J., Kose, B., and Lane, B. (2011). Dispersion Compensated Multimode Fiber. In *60th International Wire & Cable Symposium (IWCS)*, pages 410–418, Charlotte, North Carolina, USA.

Senior, J. (2008). *Optical Fiber Communications: Principles and Practice.* Prentice Hall, New Jersey.

Singer, A. C., Shanbhag, N. R., and Bae, H.-M. (2008). Electronic Dispersion Compensation– An Overwiew of Optical Communications Systems. *IEEE Signal Processing Magazine*, 25(6):110 – 130.

Telatar, E. (1999). Capacity of Multi-Antenna Gaussian Channels. *European Transactions on Telecommunications*, 10(6):585–595.

van Etten, W. (1975). An Optimum Linear Receiver for Multiple Channel Digital Transmission Systems. *IEEE Transactions on Communications*, 23(8):828–834.

van Etten, W. (1976). Maximum Likelihood Receiver for Multiple Channel Transmission Systems. *IEEE Transactions on Communications*, 24(2):276–283.

Zheng, L. and Tse, D. N. T. (2003). Diversity and Multiplexing: A Fundamental Tradeoff in Multiple-Antenna Channels. *IEEE Transactions on Information Theory*, 49(5):1073–1096.

Zhou, Z., Vucetic, B., Dohler, M., and Li, Y. (2005). MIMO Systems with Adaptive Modulation. *IEEE Transactions on Vehicular Technology*, 54(5):1073–1096.